BNL-67483

OZONE PRODUCTION AND TRANSPORT NEAR NASHVILLE, TENNESSEE: RESULTS FROM THE 1994 STUDY AT NEW HENDERSONVILLE

K. Baumann, E. J. Williams, W. M. Angevine, J. M. Roberts, R. B. Norton, G. J. Frost, F. C. Fehsenfeld, S. R. Springston, S. B. Bertman, and B. Hartsell

April 2000

Published in
J. Geophys. Res.
[vol. 105, 9137-9153 (2000)]

Research by BNL investigators was performed under the auspices of the U.S. Department of Energy under Contract No. DE-AC02-98CH10886.

JOURNAL OF GEOPHYSICAL RESEARCH, VOL. 105, NO. D7, PAGES 9137-9153, APRIL 16, 2000

Ozone production and transport near Nashville, Tennessee: Results from the 1994 study at New Hendersonville

K. Baumann[1,2,3], E. J. Williams[1], W. M. Angevine[1], J. M. Roberts[1], R. B. Norton[1], G. J. Frost[1], F. C. Fehsenfeld[1], S. R. Springston[4], S. B. Bertman[5], and B. Hartsell[6]

Abstract. During the summer of 1994 the photochemical production of ozone and the relation of this production to the photochemical precursors were studied at a suburban ground site near Nashville, Tennessee. The study, which was carried out as part of the Southern Oxidant Study (SOS), investigated the ozone produced by urban outflow during one period of high photochemical activity around July 1, 1994. Estimates of the instantaneous rate of in situ ozone production, $P(O_3)$, are inferred from deviations of the photostationary state (PSS) for clear-sky conditions. The biggest contributor to the large errors in $P(O_3)$ are the systematic errors in the derived, not measured, $j(NO_2)$ levels. Ozone entrainment from aloft has been quantified by simple subtraction of calculated production and loss terms from the observed rate of ozone change. The uncertainty of this derived transport term was estimated to a factor of 2 at best and 2 orders of magnitude at worst. Entrainment provides a substantial contribution to the observed increase of $[O_3]$ (~20 ppbv h^{-1}) in the mornings between 0700 and 1000 Central Standard Time (CST being 1 hour behind LT) when advection can be neglected. An average entrainment velocity of 1.5-2 cm s^{-1} agreed within 30 to 50% with a result found from another, completely independent study. $P(O_3)$ dominates the observed $[O_3]$ increase from 1000 CST until early afternoon, when entrainment weakens and even turns into an effective ozone loss term due to cloud venting processes. The July 1 case clearly demonstrates that the morning ozone entrainment occurs on a more regional scale covering the entire study area, whereas the midday ozone exceedance was spatially more confined to the area covered by the advective outflow of the chemically processed Nashville urban plume. The data show that the entrained $[O_3]$-rich air aloft is the remnant of the previous day's local ozone buildup and subsequent nocturnal advective redistribution.

1. Introduction

Elevated and potentially harmful levels of ozone (O_3) are being found in many areas of the southeastern United States during summer. There is substantial evidence from field measurements and model calculations that most of this O_3 is being produced photochemically by reactions involving the precursor compounds: carbon monoxide (CO), volatile organic compounds (VOC), and nitrogen oxides (NO_x=NO+NO_2) [*Research Triangle Institute (RTI)*, 1975; *Vukovich et al.*, 1977, 1985; *Cleveland et al.*, 1977; *Spicer et al.*, 1979; *Wolff and Lioy*, 1980; *Fehsenfeld et al.*, 1983; *Kelly et al.*, 1984; *Liu et al.*, 1987; *National Research Council (NRC)*, 1991].

Nashville, Tennessee, is an example of a midsize urban area in the southeastern United States that is experiencing O_3 pollution episodes in the summertime. Nashville is surrounded by rural areas, which are dominated by forests and agriculture. In addition, large isolated industrial point sources are located upwind of Nashville to the west and north. The greater Nashville metropolitan area is outlined in Figure 1 along with the locations of different pollutant point sources, for example, power plants, and their 1994 emissions (D. J. Lokey, Tennessee Valley Authority (TVA), personal communication, 1997). The DuPont chemical plant data reflect emissions from before 1994 [*Environmental Protection Agency (EPA)*, 1989]. Nashville itself is a source for VOC, CO, and NO_x. For comparison, 1994 NO_x and CO emissions from traffic-related sources within the greater Nashville metropolitan area (i.e., Davidson county) were estimated to be 108 and 857 x 10^{23} molecules/s respectively (C. Cardelino, Georgia Institute of Technology (GIT), personal communication, 1997). Although Nashville is reasonably isolated from other urban areas, the power plants contribute significant emissions of NO_x to the region; for example, the Cumberland power plant to the west emits about 5 times more NO_x. In addition, forests are a major source of biogenic VOC such as isoprene. In the summertime, oxidation of these primary pollutants leads to the formation of secondary pollutants such as O_3.

[1]Aeronomy Laboratory, NOAA, and Cooperative Institute for Research in Environmental Science, University of Colorado, Boulder, Colorado.
[2]Also at Advanced Study Program, National Center for Atmospheric Research, Boulder, Colorado.
[3]Now at School of Earth and Atmospheric Sciences, Georgia Institute of Technology, Atlanta.
[4]Environmental Chemistry Division, Brookhaven National Laboratory, Upton, New York.
[5]Department of Chemistry, Western Michigan University, Kalamazoo.
[6]Atmospheric Research and Analysis, Inc., Plano, Texas.

Paper number 1999JD901017.
0148-0227/00/1999JD901017$09.00

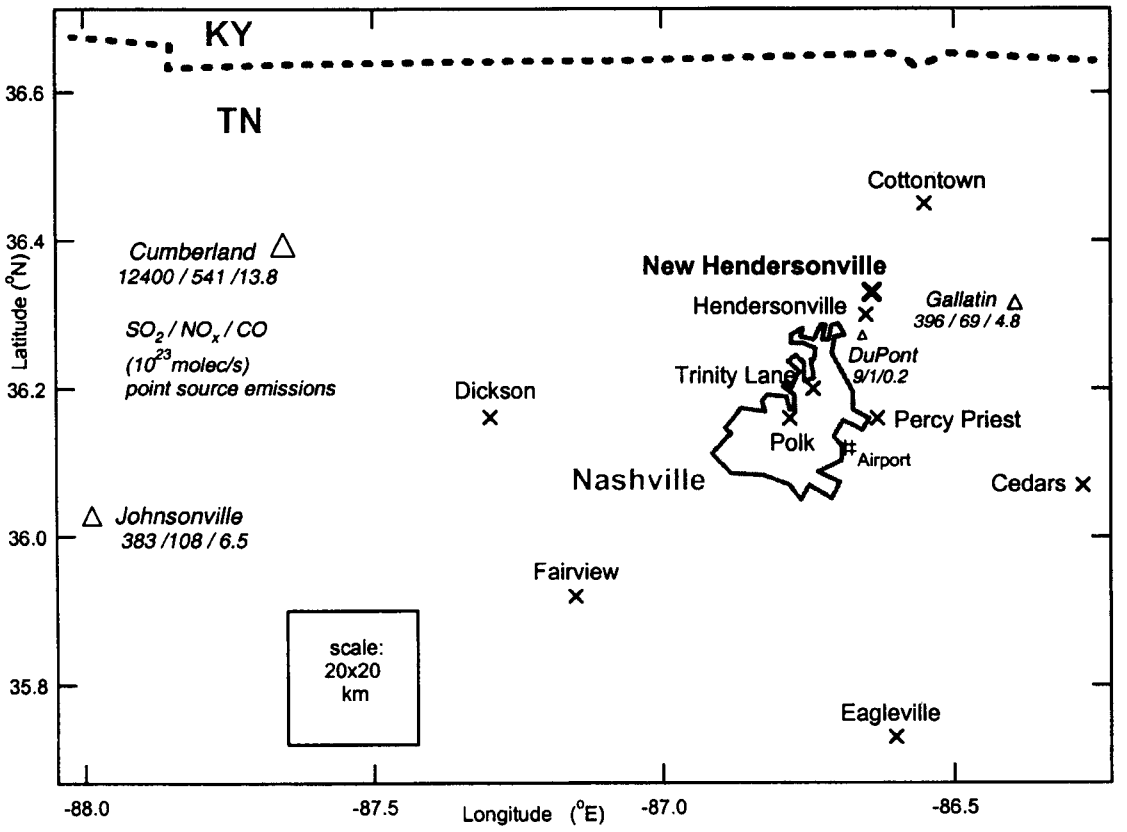

Figure 1. Map of the greater Nashville, Tennessee, area, showing locations of the principal ozone monitoring stations and major emission point sources with their SO_2, NO_x, and CO emission strengths.

The Nashville metropolitan area, with a population of approximately one million, has a long history of O_3 pollution problems. Like most nonattainment areas, Nashville is classified by the EPA as having a moderate O_3 problem: its National Ambient Air Quality Standards (NAAQS) design value is 138 ppbv. Between 1988 and 1994, O_3 mixing ratios have been monitored at several sites in and around the Nashville metropolitan area as shown in Figure 1. Over this period, 121 hourly averaged O_3 mixing ratios above the 120 ppbv NAAQS standard were recorded at these stations. However, during this period the highest O_3 levels were recorded at the Hendersonville station, which is 19 km north-northeast of downtown Nashville.

For this reason, the Southern Oxidants Study (SOS) elected to establish a highly instrumented monitoring site nearby. This location was designated by SOS as New Hendersonville and was operated during the study periods in summers of 1994 and 1995 in order to understand the photochemical and meteorological processes that lead to the elevated O_3 levels in Nashville [cf. *Meagher et al.*, 1998]. In addition, during the 1994 study, rigorous intercomparisons of the methods used to measure NO_y were carried out at the site [*Williams et al.*, 1998]. NO_y includes NO_x and its more (photochemically) stable oxidation products nitric acid (HNO_3), aerosol nitrate (NO_3^-), peracetic nitric anhydride (PAN), methylacrylic nitric anhydride (MPAN), and peroxypropionic nitric anhydride (PPN). This afforded the opportunity for the state-of-the-art $NO/NO_x/NO_y$ measurements, which were involved in the intercomparison, to provide an excellent set of high quality reactive nitrogen oxide measurements during this period.

In addition to NO_y, a variety of other photochemically active trace gas constituents were measured at New Hendersonville in 1994. This allowed the study of the photochemical production of O_3 and the relationships of O_3 production to O_3 precursors that are present in the urban outflow during periods of high photochemical activity and stagnant high pressure, which are the typical conditions leading to high O_3 concentrations in the southeastern United States.

This paper will identify periods when O_3 exceeded the older NAAQS 120 ppbv 1-hour standard and the new 80 ppbv 8-hour standard during the study period in 1994. The primary focus will be on the chemical and meteorological measurements made at the New Hendersonville site where the most extreme exceedance occurred on July 1. A subsequent detailed analysis will then examine how the various sources of the photochemical precursors of O_3 outlined above might have contributed to that episode. The rates of photochemical ozone production, loss, and surface deposition are estimated and compared to the observed net rate of ozone change. Hence we derive implications for ozone transport processes such as entrainment, advection, and cloud venting, and their importance for the observed $[O_3]$ exceedances.

2. Meteorological Measurements

Wind speed and direction, dew point and air temperatures, air pressure, precipitation, and solar UV irradiance (Eppley) were measured at the top of a 10 m scaffolding tower. Data were acquired at 1 s intervals and averaged to 1 min points. The photolysis rate coefficients, or $j(NO_2)$ values, were calculated using the Madronich radiative transfer model (S. Madronich et al., manuscript in preparation, 1999), which is based upon the Stamnes discrete ordinates model modified to solve the radiative transfer equation in pseudo-spherical coordinates [*Dahlback and Stamnes*, 1991]. The discrete ordinates code was run with eight streams. The surface albedo was assumed to be 5%, and the total aerosol optical depth was parameterized in terms of visual range. The model assumes a constant visual range of 25 km for the lowest 2 km, a logarithmically decreasing aerosol optical depth above this, as well as a single scattering albedo of 0.99 and an asymmetry parameter of 0.61, which are both wavelength-independent. The $j(NO_2)$ values were then scaled linearly by the flat-plate Eppley-UV (290-385 nm) measurements and by their ratio to the radiative transfer model clear-sky irradiance to account for the actual cloud and aerosol effects on $j(NO_2)$. This scaling helps to correct for any errors made by the visual range assumptions. A 915 MHz boundary layer wind profiler was deployed at the site and acquired 30 min average wind speed and direction vertical profiles at a resolution of about 60 m. It used wind-induced Doppler shifts in one vertical and four off-zenith beams. The radar's backscatter profiles obtained from refractive-index inhomogeneities associated with atmospheric turbulence were used to estimate the daily evolution of the convective boundary layer (CBL) and the extent of its mixing depth z_i [*White*, 1993; *Angevine et al.*, 1994a, b]. The wind speed measurements at the lowest range gate, that is, 160 m above ground level (m agl) provided an estimate for the upper limit of the depth of the nocturnal inversion.

3. Chemical Measurements

All chemical measurements were made on the tops of standard construction scaffolding towers at about 9 m agl. The data were acquired at 1 Hz and averaged to 1 min points unless noted otherwise. The detection limits, the time intervals over which the measurements were averaged, and precision and accuracy estimates of each technique are summarized in Table 1. The individual techniques are described briefly in the following.

Three independent channels operated simultaneously to measure NO, NO_x (NO plus NO_2 photolytically converted to NO in Xe arc UV light [*Kley and McFarland*, 1980]), and NO_y. The NO_y was converted with an Au tube heated to 300°C in the presence of CO [*Fahey et al.*, 1986]. PAN, MPAN, and PPN were measured every 20 min by gas chromatography (GC) with electron capture detection (ECD) [*Williams et al.*, 1997]. Aerosol nitrate (NO_3^-) and HNO_3 were measured by Teflon/Nylon filter pair sampling followed by extraction and analysis via ion chromatography [*Norton et al.*, 1992].

A fast flow tube with a filtered inlet at the top of the tower delivered air to a manifold that was used to sample air for the measurement of O_3, CO, and sulfur dioxide (SO_2) with instruments located inside the Aeronomy Laboratory trailer.

Table 1. Measured Species, Detection Limits (DL), Precision and Accuracy of the Measurements for Given Time Intervals

Species	DL	Time Interval	Precision	Accuracy %
NO	5 pptv	10 s	±15%	±20
NO_2	20 pptv	10 s	±20%	±20
NO_y	50 pptv	10 s	±20%	±30
PAN	3 pptv	1 min	±5%	±20
MPAN	3 pptv	1 min	±5%	±30
PPN	3 pptv	1 min	±5%	±30
HNO_3	3 pptv	1 hour	±20%	±20
NO_3^-	3 pptv	1 hour	±20%	±20
O_3	2 ppbv	1 min	±2 ppbv	±5
CO	20 ppbv	1 min	±10%	±10
SO_2	150 pptv	1 min	±10%	±10

O_3 was measured using a pressure- and temperature-compensated commercial UV absorption instrument (model 1108, Dasibi Corporation). CO was measured by a gas filter correlation, nondispersive infrared absorption instrument (model 48s, Thermo Environmental Instruments) that was modified according to *Parrish et al.* [1994] for frequent zero checks and standard addition calibrations. The plumbing setup allowed the zero trap to be conditioned to changing levels of ambient water vapor, which is known to be a major interferent. The signal output was pressure- and temperature-compensated. SO_2 was measured by a commercial, pulsed UV fluorescence instrument (model 43s, Thermo Environmental Instruments). Since the instrument measurement principle is known to be sensitive to organic hydrocarbons (HC), the efficiency of the internal HC removal from the sampled air through a semipermeable wall was enhanced by introducing activated carbon into the flow of the low-[HC] side of the wall, that further increased the [HC] gradient across the wall.

4. Results

4.1. Episodes When Violations of the NAAQS O3 Standards Occurred

The O_3 data to which the National Ambient Air Quality Standards (NAAQS) are applied are based on 1-hour averages of O_3 mixing ratios measured at surface monitoring stations. The standard set by the 1967 Clean Air Act designated areas as out of compliance if more than three 1-hour averages of O_3 exceeded 120 ppbv within a 4-year period. In July 1997, EPA has revised this standard to that the annual fourth-highest daily maximum 8-hour ozone concentrations (i.e., 8-hour running means of 1-hour O_3 averages) not to exceed 80 ppbv within 3 years. Figure 2 shows that during the 1994 study at the New Hendersonville site the current 120 ppbv standard was violated (though not officially) one time on July 1. The 8-hour 80 ppbv standard was violated three times: June 22, July 1, and July 19. However, the July 19 episode does not show a complete data record for O_3, and the running mean does not represent a full 8-hour period in the instances when the trace exceeds 80 ppbv. On the other hand, the data for July 1 show that the 80 ppbv standard was violated for 6 consecutive hours while the 120 ppbv standard was violated

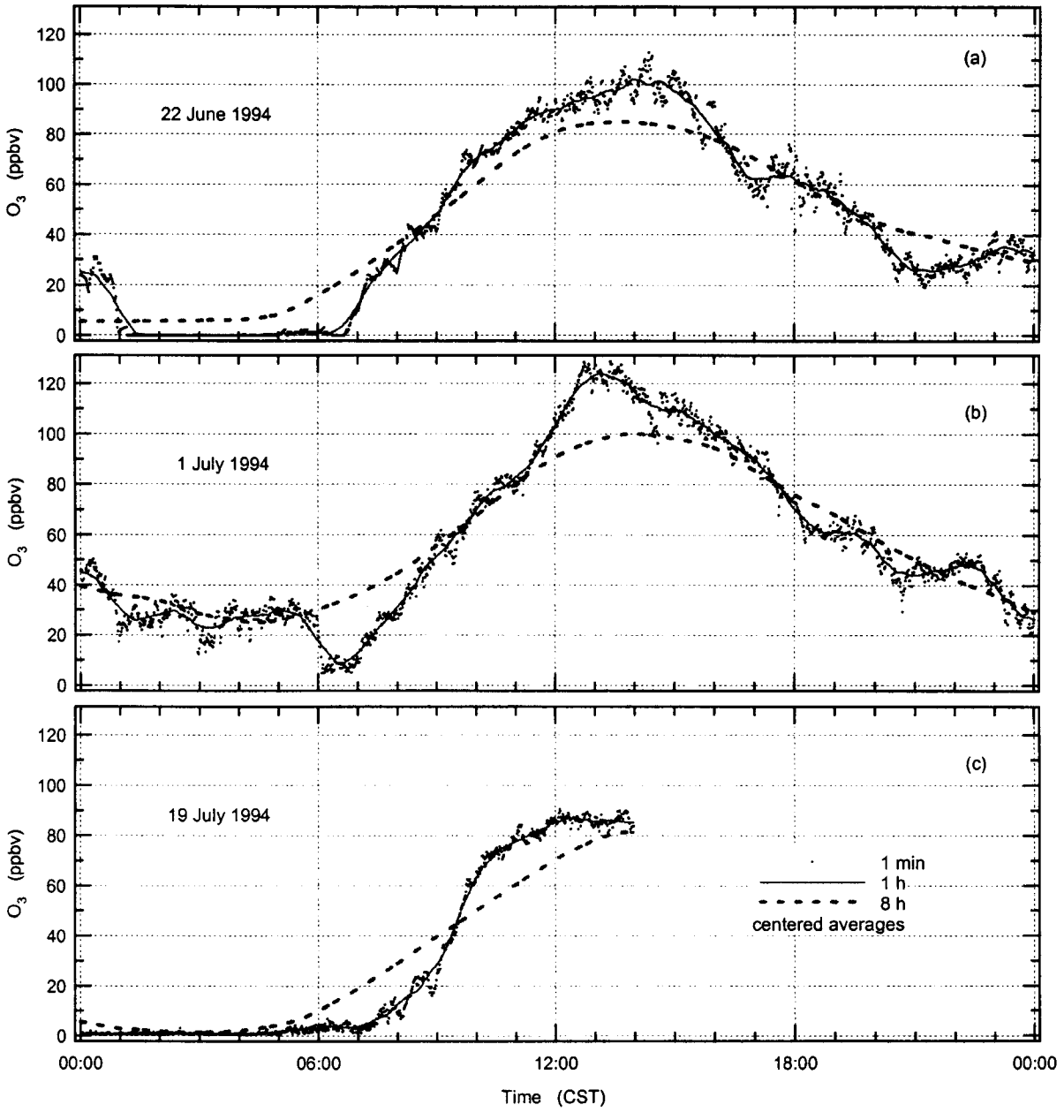

Figure 2. (a) Plot of 1 min O_3 mixing ratios (dots), running 1-hour averages (solid grey line), and running 8-hour averages of 1 min O_3 data (dashed grey line) for June 22, 1994, at the New Hendersonville site. (b) Same as Figure 2a, except for July 1, 1994. (c) Same as Figure 2a, except for July 19, 1994.

for only 1 hour. Thus it appears that the newer, proposed, standard is more stringent than the older, existing, standard [*St. John and Chameides*, 1997]. The rest of this paper will present a detailed analysis of the high O_3 episode on July 1.

4.2. Meteorological Conditions for the July 1 High O_3 Episode

The 850 mbar constant pressure contour maps showed relatively small pressure gradients across the eastern United States on June 28 due to a stationary high-pressure system over the Gulf of Mexico and a low stalled over central Ontario, Canada. On July 1 the high-pressure system settled over Alabama. This resulted in almost stagnant conditions (with changing wind directions from northwest to southwest over Tennessee) over the southeastern United States. During the course of July 2, a high-pressure cell formed over the northern Midwest, and a low replaced the disappearing high over the Gulf of Mexico. Thus this 5-day period was characterized by generally calm conditions with small pressure gradients and no frontal activity or passages.

Data for wind direction and speed at 10 and 550 m agl, air and dew point temperature (and derived H_2O mixing ratios), air pressure, UV radiation (290-385 nm and $j(NO_2)$ values derived from the Eppley data), and the evolution of the boundary layer height (z_i) are depicted in Plate 1. The CBL

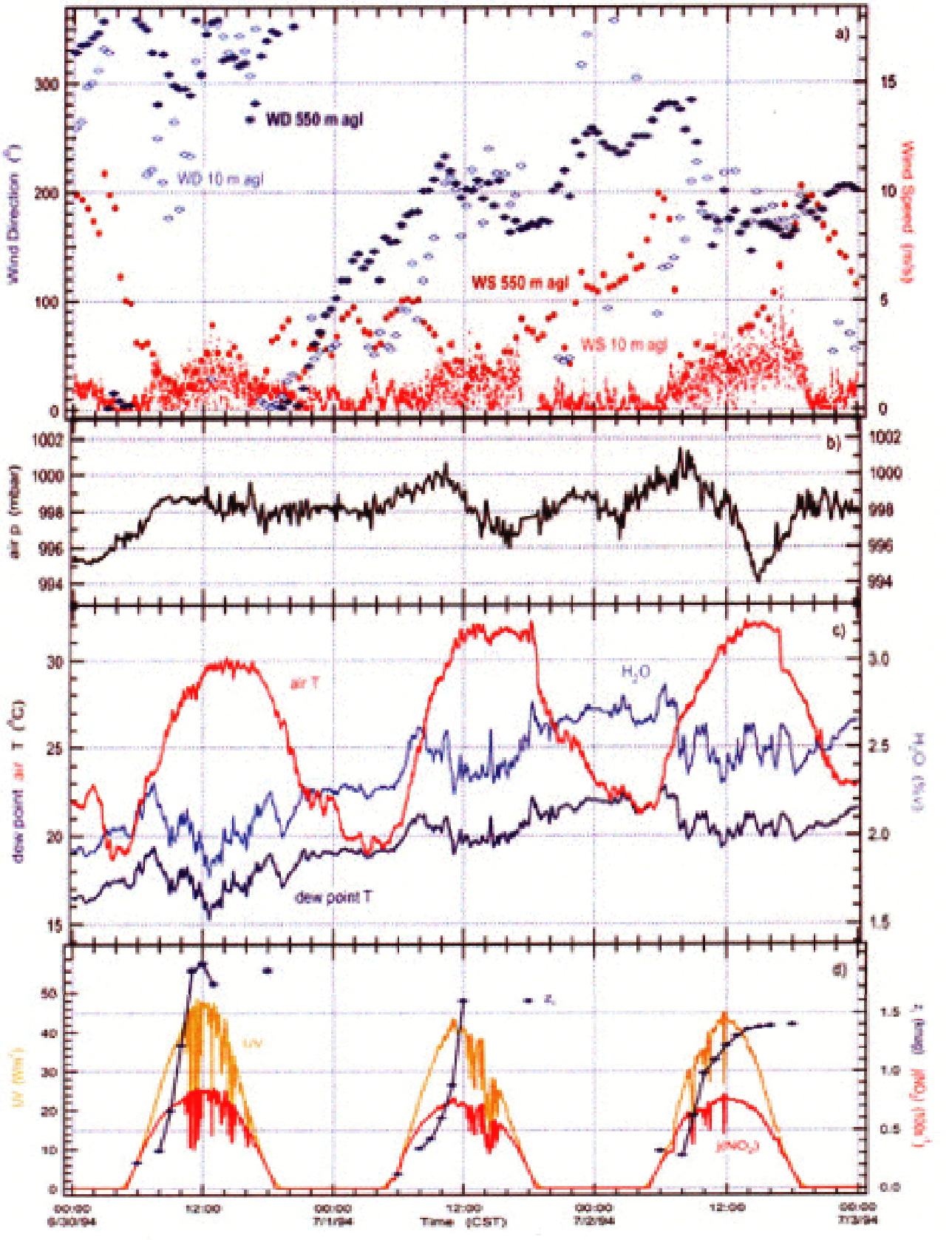

Plate 1. Variations of (a) the wind direction and speed at 10 and 550 m agl, (b) the surface air pressure, (c) the air and dew point temperatures and derived H_2O mixing ratio, and (d) the Eppley UV data and derived $j(NO_2)$ values and the CBL mixed height z_i derived from wind profiler data and radiosonde soundings over the period June 30 to July 2, 1994, at New Hendersonville.

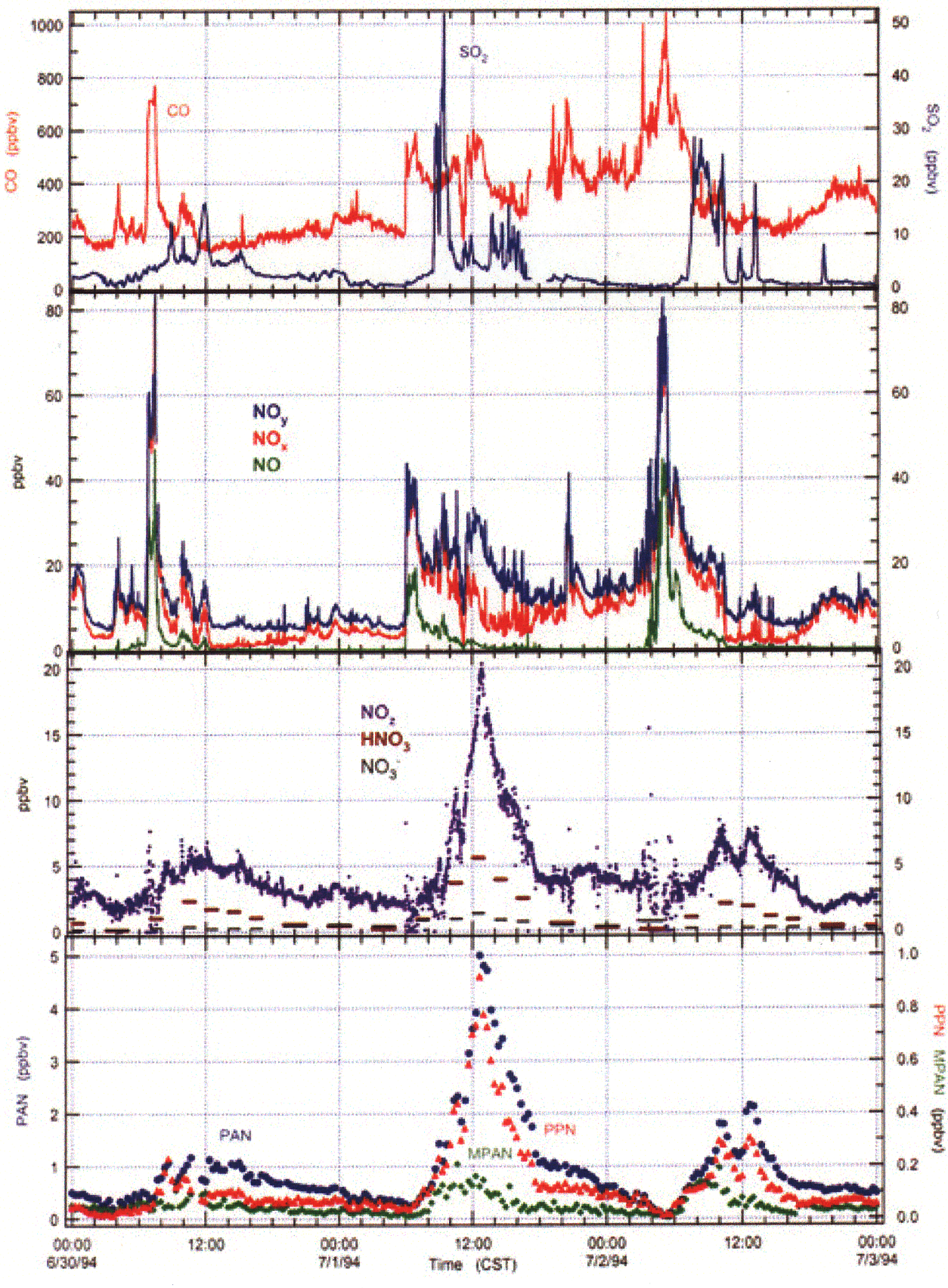

Plate 2. Traces of various chemical parameters measured at New Hendersonville on July 1, 1994, and the 2 neighboring days for comparison with Plate 1.

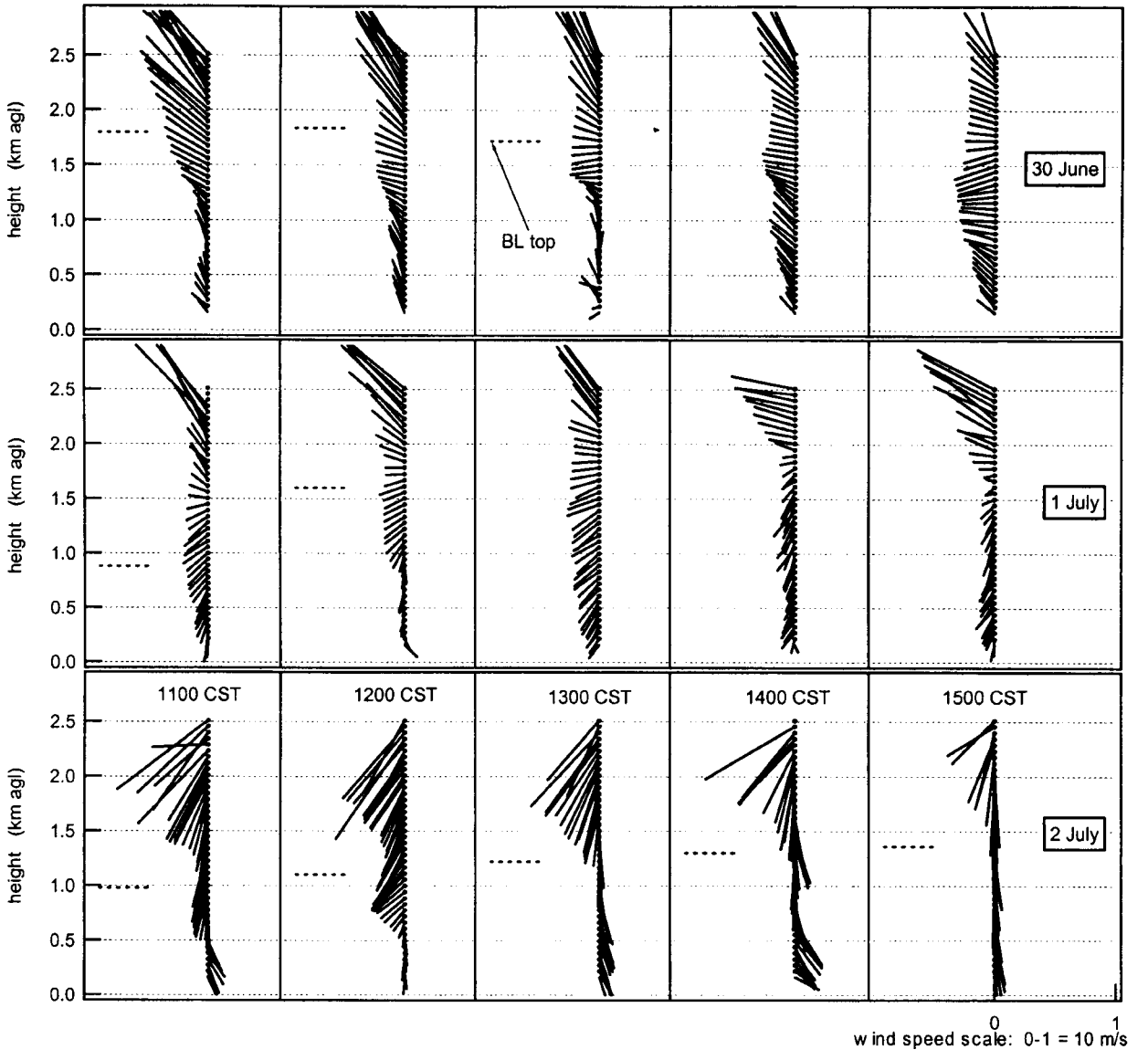

Figure 3. Comparison of profiler wind profiles for same midday periods on (top) June 30, (middle) July 1, and (bottom) July 2, 1994.

heights at 0600 and at 1800 CST were retrieved from National Weather Service data and provided by the Forecast Systems Laboratory (FSL) of NOAA (M. Govett, NOAA-FSL, personal communication, 1997). Since the CBL was breaking down by 1800 CST, the z_i quoted at that time indicates the height of the residual mixed layer, while z_i reported at 0600 CST indicates the maximum depth of the nocturnal inversion layer. During this 3-day period, surface winds were low, reflecting the influence of the stagnant high-pressure system. During the first half of the first day (June 30), the wind was from northwesterly directions. The wind direction progressively veered northerly and easterly during the second half of June 30. The wind kept veering to more southerly directions during the morning of the second day (July 1). Between 1000 and 1700 CST the wind directions both at the surface and at 550 m agl indicated constant southwesterly flow. Surface winds were calm until sunrise of July 2. However, at 550 m agl the wind speed was slowly increasing, and the flow direction was slowly rotating to the west. All this indicated a continuous influence of the urban outflow until ~0700 CST on July 2. Then the flow scheme settled to a relatively homogeneous southeasterly direction. The sky during the first 2 days was mostly clear in the morning with increasing scattered to broken clouds in the afternoons, with an inverse pattern showing on July 2 when the sky cleared up around noon. Temperatures varied between nocturnal lows of 19-22°C, to daytime maxima ranging between 30° and 32°C. Humidity levels reached saturation almost every night.

The relatively constant southwesterly flow from Nashville during most of the day on July 1 is illustrated by Figure 3 (center) which shows wind profiles between 1100 and 1500 CST in comparison with the day before (top) and the day after

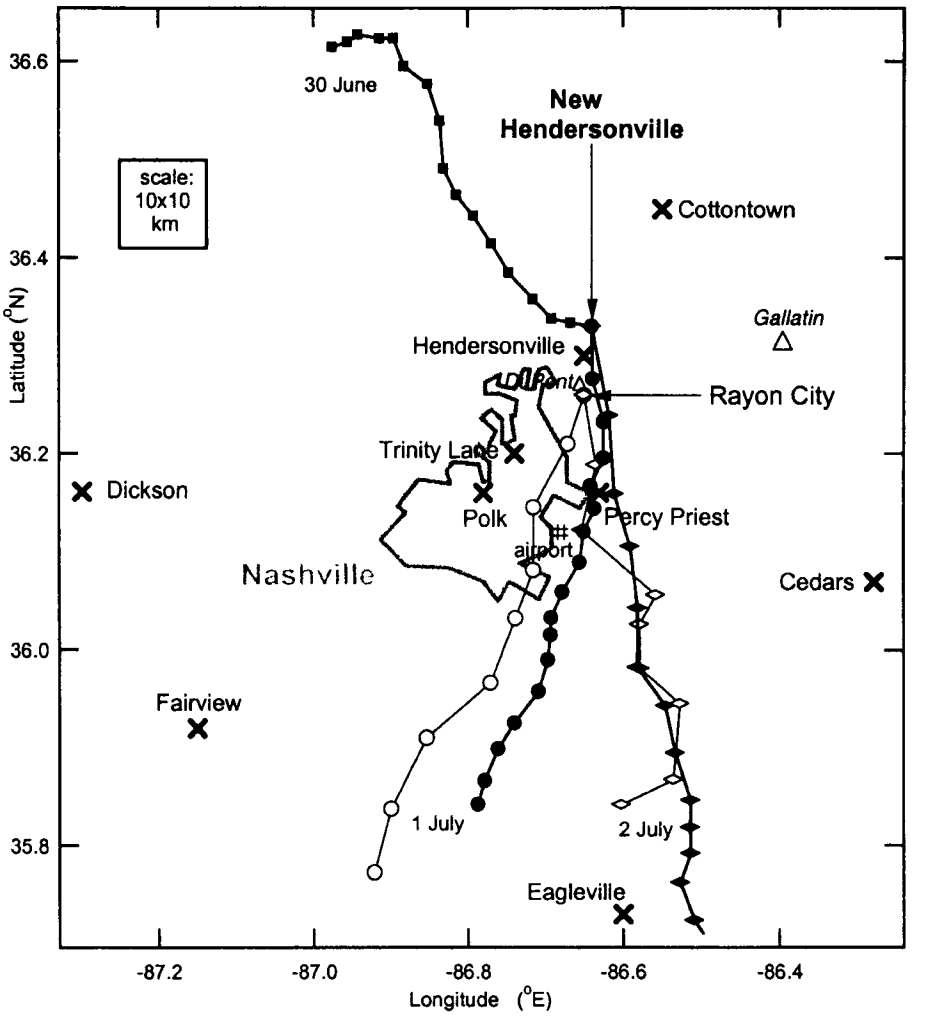

Figure 4. Map of the region surrounding Nashville with back trajectories denoting air mass transport in the lower to mid-CBL arriving each at 1700 CST; solid symbols, New Hendersonville 30 min; open symbols, Rayon City 60 min time increments.

(bottom) July 1. This time window was chosen because it represents the period of most intense photochemical activity discussed in the following section. The abscissa shows the scale for the wind speeds in m s^{-1} represented by the lengths of the vectors that point to the direction where the wind is coming from (i.e., left is from the west). Besides the constant southwesterly flow throughout the CBL, the July 1 case stands out because of the very small gradient in wind speed compared to the other 2 days. Boundary layer heights determined from the profiler are shown in Figure 3 (dashed lines) for hours when they could be confidently determined. Missing CBL heights indicate the presence of scattered to broken cumulus clouds, which make CBL height determination (and the definition of the CBL height itself) uncertain.

4.3. Chemical Measurements During the July 1 High O_3 Episode

Mixing ratios of CO, SO_2, NO, NO_x, NO_y, NO_z (NO_z=NO_y-NO_x), NO_3^- and HNO_3 (determined from 1-hour filter samples for this period), PAN, PPN, and MPAN are shown in Plate 2. The individually measured NO_y species HNO_3, NO_3^-, PAN, PPN, and MPAN correlated with [NO_z]. The midday maxima in [MPAN] were not as pronounced as for [PAN] and [PPN]. In the presence of NO_x, MPAN results from photochemical processing of biogenic VOC (BVOC, primarily methacrolein, an isoprene oxidation product), and PPN is the photochemical oxidation product of anthropogenic VOC (AVOC, namely, propanal, propane, and larger alkanes). *Roberts et al.* [1998] showed, first, that relatively strong isoprene sources in Nashville itself caused the substantial increase in [MPAN] on July 1 relative to the day before when the site was influenced by air masses from the north; second, that the study's highest [PPN] observed on July 1 were caused by AVOCs emitted in the Nashville metropolitan area and transported with the urban plume. Because both BVOC and AVOC sources are small in the less forested and less urbanized region north of Nashville, very low mixing ratios of these PAN-type compounds were measured the day before (June 30) when the wind was from the north and northwest.

5. Discussion

In the following discussion, the New Hendersonville data are used to study some of the features of O_3 photochemistry and transport in this urban environment. Ground measurements are used to establish an ozone budget and to determine the net rate of $[O_3]$ change which is compared with the calculated gross production rate and estimated O_3 loss rate via photochemistry and deposition. The effects of transport on the observed changes in ozone abundance within the CBL are then determined.

5.1. Spatial Extent of the July 1 High O_3 Episode

Estimates of air mass back trajectories for the 3-day period of this study are shown in Figure 4. These trajectory estimates were derived by averaging the lowest nine range gates of the wind profiler (between 160 and 608 m agl) as a function of time. A similar profiler was deployed at Rayon City, about 7 km due south and 30 m lower in elevation than New Hendersonville. This profiler was operational beginning July 1 (A. B. White, Environmental Technology Laboratory (ETL), NOAA, personal communication, 1997), and data from it were averaged similarly to those of the New Hendersonville instrument. By assuming the same wind field applied to the entire region, the average speed and direction from the profilers could be used to derive the air mass history within the CBL above the two sites terminating at 1700 CST. The trajectory arriving at New Hendersonville has a time resolution of 30 min; the one at Rayon City is incremented into 1-hour intervals so that both span over the total time period from 0900–1700 CST. It is evident that the constant southwesterly flow on July 1 was not limited locally to New Hendersonville and that it lasted at least until 1530 CST.

The O_3 data of all monitoring sites covering a larger region around Nashville are shown together with the O_3 mixing ratios observed at the New Hendersonville site in Figure 5. The special CBL wind conditions on July 1 made (old) Hendersonville, New Hendersonville, and Cottontown be located downwind (Figure 5a), and Cedars, Eagleville, Fairview, and Dickson upwind or away from the urban plume of Nashville (Figure 5c). The northwesterly flow on June 30 of course placed Cedars downwind from Nashville, although not directly in the plume center. Some features in the $[O_3]$ traces seem to be common to all the sites. For example, all sites showed a rapid $[O_3]$ increase between 0600 and 0900 CST on all 3 days; this is indicative of a regional feature in the O_3 levels. Many of the stations exhibit significant O_3 depletion at night. Clearly, the urban stations (Figure 5b) and the suburban sites (the Hendersonvilles, Cottontown, and Percy Priest) will experience O_3 titration by local emissions of NO in addition to surface deposition losses. The latter is likely the dominant nighttime loss at the more rural locations (Figure 5c). The most striking feature of Figure 5 is the locally limited character of the high $[O_3]$ episode at the Hendersonvilles and Cottontown on midday of July 1 when all three sites were impacted by the Nashville urban plume with Cottontown being farthest downwind. Note that the stations Polk, New Hendersonville, and Cottontown lie almost exactly in a straight line along which the mean outflow of the urban plume occurred. The Polk station is on top of the James K. Polk building, 110 m agl, on the corner of Fifth and Deadrick Avenues in downtown Nashville (see Figure 4). Owing to the distance from the ground, this measurement has a greater "footprint" and therefore represents a typical ozone level of the greater Nashville urban area. Assuming homogeneous mixing and steady state conditions in the region (a greatly idealized simplification), a net ozone production rate can be estimated for the urban plume from

$$P(O_3)_{net} = ([O_3]_{NH} - [O_3]_{Polk}) \times AF / D,$$

where AF is the airflow derived from the trajectory and projected onto the direct distance D between New Hendersonville (NH) and Polk. Under the same assumptions a net ozone loss rate $L(O_3)_{net}$ can be determined in a similar fashion for an air parcel that travels in the dispersing plume from New Hendersonville to Cottontown. Both terms are depicted in Figure 5d showing a steady increase before noon to a nominal maximum at 1300 CST of 8.3 ppbv h^{-1} net ozone production upwind, and 5.9 ppbv h^{-1} net ozone loss downwind from New Hendersonville. If in situ loss and mixing rates were the same along the entire plume trajectory a maximum photochemical gross production rate could be estimated by the sum of both rates, that is, ~14 ppbv h^{-1} at 1300 CST. Figure 5d shows also plume ozone production rates $P(O_3)_{net}$ calculated the same way for the other 2 days assuming Cedars downwind from Polk on June 30 and New Hendersonville downwind from Percy Priest on July 2.

Comparing the July 1 case with the day after (Plates 1 and 2) shows that the close vicinity of pollution sources made the measured data at the site very sensitive to changing flow conditions, in particular to wind direction and atmospheric turbulent mixing. Continuous southwesterly flow was maintained well into the afternoon on July 1 causing elevated levels of CO and NO_x throughout this day. On July 2, at around 0730 CST, a clear shift to south-southeasterly wind directions brought in air masses high in $[SO_2]$, lower in $[NO_x]$, and lowest in [CO] that were indicative of the Gallatin power plant to the east. The most significant difference to July 1, however, occurred when the site remained under the influence of more southeasterly flow for the rest of the daytime period of July 2.

Finally, $[O_3]$ data from the NOAA WP-3D Orion research aircraft (P3) are used to examine the vertical extent of mixing in the CBL. Although no aircraft flights were conducted on July 1, flights took place 1 day before and 1 day after. On June 30 the P3 ascended between 1204 and 1213 CST from a flight altitude of about 720 m agl up to 1920 m agl at a horizontal distance of about 60 km to the west-northwest (upwind) of New Hendersonville. This vertical profile was the one flown closest to the ground site this day. The $[O_3]$ aloft varied between 58 and 65 ppbv up to an altitude of 1490 m agl and then declined rapidly to around 45 ppbv at higher altitudes. The 1490 m agl marked z_i, the height of the CBL. During these 9 min, the New Hendersonville $[O_3]$ increased from 57 to 67 ppbv. The agreement between both data sets points to a CBL that was well mixed. Surface winds were from the northwest; therefore the ground site was not directly impacted by the urban plume. However, on July 2, around noon, surface winds were from the south and from south-southeasterly directions at higher altitudes. Between 1248 and 1251 CST the aircraft ascended from 410 to 1960 m agl at about 60 km northwest of New Hendersonville. The top of the CBL, z_i, was about 1120 m agl, and O_3 levels varied between 65 and 69 ppbv below this altitude, again indicating well mixed conditions. At this time, however, the New

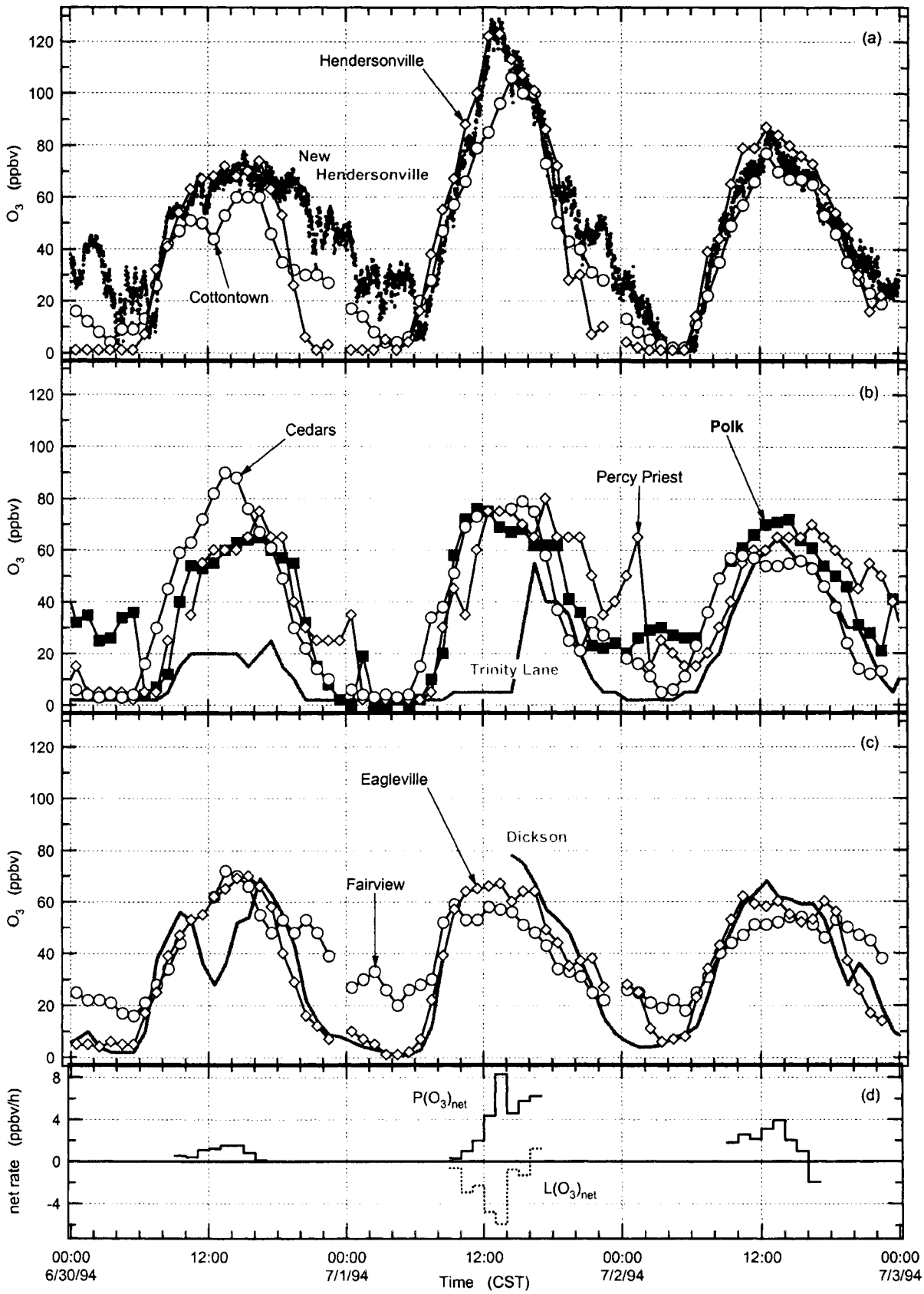

Figure 5. Ozone measured at New Hendersonville (dots) and at the other ground stations labeled in Figures 1 and 4 on July 1, 1994, and the 2 neighboring days for comparison with Plates 1 and 2. Bottom panel shows net ozone production and loss rates within the urban plume (see text for details).

Hendersonville [O_3] was at a maximum of 80-85 ppbv. This was caused by the influence of the urban plume that was moving to the north, while the P3 vertical ozone profile was flown to the west, outside the plume. However, on both days the P3 did record maximum [O_3] in the direct outflow of the urban plume, similar to that seen in the New Hendersonville data: on June 30, under conditions of higher wind speeds and deeper CBL than on July 1, the maximum [O_3] encountered by the P3 was 92 ppbv at 1511 CST, 980 m agl and 20 km downwind, and 98 ppbv on July 2 1144 CST at 750 m agl and 35 km downwind from the Nashville city center (D. D. Parrish, M. Trainer, and G. Hübler, Aeronomy Laboratory, NOAA, personal communication, 1997). The reasons for the higher maximum P3-[O_3] on July 2 can be seen both in the shallower CBL and in the entrainment of higher [O_3] from the previous day's ozone pollution. The importance of preserving ozone in nocturnal residual layers that are removed and isolated from the surface, and the role of vertical and horizontal transport, that includes entrainment, cloud venting, and advection, as an effective mechanism for shaping the observed ozone levels is discussed in the following sections. Clearly, vertical and horizontal transport must be considered for the [O_3] observations at New Hendersonville, in addition to photochemistry.

5.2. Principal Factors Affecting O_3 Observed at New Hendersonville

A simple budget analysis is performed by equating the changes in [O_3] observed at New Hendersonville to the principal production and loss terms:

$$d[O_3]/dt = P(O_3) + L(O_3) + L_{dep} + T. \quad (1)$$

The procedures and uncertainties of deriving these production and loss terms are described in the following. A nonanalytical descriptive summary of these procedures has been presented by *Baumann et al.* [1999].

The first term on the right side of equation (1) is estimated from the photostationary state relationship of NO, NO_2, and O_3. Consider the two terms on the right-hand side of the following equation:

$$P(O_3) = [NO]\, k_{2i}[R_iO_2] = j(NO_2)[NO_2] - k_1[O_3][NO], \quad (2)$$

where $j(NO_2)$ is the photodissociation rate of NO_2 and k_1 is the rate constant for reaction of O_3 with NO. In the absence of other processes, the production and loss of O_3 defined by the two right-hand terms above will balance and yield a photochemical stationary state (PSS) for which there will be no net O_3 formation. However, reactions of OH with CO and VOC lead to the formation of HO_2 and a variety of organic peroxy radicals, R_iO_2. The reaction of NO with these peroxy radicals (middle term of equation (2), where the k_{2i} are rate coefficients for reactions of NO with any number of peroxy radicals [*Atkinson*, 1990; *Peeters et al.*, 1992]) perturbes the PSS, resulting in an instantaneous gross in situ ozone production rate, assuming NO in steady state. Reactions implied by equation (2) are considered the only ones that significantly alter the PSS and lead to O_3 production in the sunlit troposphere [e.g., *Parrish et al.*, 1986; *Ridley et al.*, 1992; *Frost et al.*, 1998, and references therein]. To ensure that the primary assumption of photostationary state, that is, rapid interconversion between NO and NO_2 (~1 min), was correct, the data here were restricted to (1) strictly coincident 1 min data without interpolations; (2) periods with high light levels under mostly clear-sky conditions, with $j(NO_2) > 0.005$ s^{-1}; and (3) changes of any of the quantities smaller than 20% of the previous 1 min value. According to equation (2) the highest production rates should occur when the product of [NO] and $k_{2i}[R_iO_2]$ reaches a maximum. On July 1, for example, [NO] decreased between 0700 and 1100 CST from about 18 ppbv to less than 2 ppbv, while its fraction of [NO_x] decreased from 45% to less than 20% (Plate 2). Ozone (and radical) levels built up simultaneously as [HNO_3] increased, corresponding to NO_x oxidation, in particular via NO_2 reaction with OH. This calculation of $P(O_3)$ (the two right-hand terms of equation (2)) is the difference between two quantities of similar magnitude. This can lead to significant errors [*Chameides et al.*, 1990; *Kleinman et al.*, 1995] that we estimate as follows.

Values for $j(NO_2)$ were calculated for clear-sky conditions using the radiative transfer model and subsequently scaled by Eppley-UV measurements to account for cloud effects, as described above. On the basis of 20% errors in the cross sections and quantum yields of NO_2 [*DeMoore et al.*, 1994], an uncertainty of 10% in the Eppley measurement itself [*Shetter et al.*, 1992], and a conservative estimate of 20% for any errors in using a linear scaling of modeled $j(NO_2)$ by the ratio of the measured and modeled irradiance, we have estimated the $j(NO_2)$ uncertainties in accuracy at 30%.

Uncertainties in the accuracy of the NO and NO_2 measurements utilizing the chemiluminescence detection (CD) technique of the instrument used in this study were estimated at ±(19% +8 parts per trillion by volume (pptv)) for NO and ±(22% + 5 pptv) for NO_2 [*Williams et al.*, 1997]. These estimates were determined via propagation of errors introduced by the calibration standard, the mass flow controllers, and instrument background. The main difference and improvement of the instrument used in this study was that it allowed simultaneous measurement of NO_x in a separate channel from NO, therefore not requiring interpolation of the NO signal in order to derive NO_2. Hence the accuracies for both the NO and the NO_2 measurements here are estimated conservatively at ± 20% (see Table 1). The introduction of zero air, that is, ultrapure, NO_x–free air to the inlet, resulted in a detectable signal known as "instrument artifact" for both NO and NO_2, and represents a systematic error for this technique. However, it is accounted for in the data reduction, therefore contributing only little to the overall uncertainty of the reported data on a random basis. For example, during the 3-day period around July 1, the NO artifact averaged 16 ± 4 pptv and was 98 ± 7 pptv for NO_2, with variations expressed as single standard deviations. The uncertainty of the [NO] calibration standard had been determined by a round-robin evaluation among all participants to be ±3.5%. The uncertainty in the calibration of the sample air and calibration gas mass flow controllers is estimated to be 2% for each set point, respectively. Thus the total systematic error in the calibration system can be estimated at ±5% and falls well within the total estimated ±20%. NO_3 and HONO are potential interferences for the NO_2 measurement in that they rapidly and most efficiently photolyze in the broadband Xe UV spectrum. This is mainly the reason why their atmospheric abundance relative to NO_2 during middays is rather insignificant, which are the daytime periods subject to investigation of this work.

$P(O_3)$ values were calculated for 1 min time intervals for which coincident measurements of the independent input parameters had been reported that met the above screening criteria. Of all the input variables measured, NO and NO_2 were the least complete. In order to maximize the resulting number of 1 min $P(O_3)$ data, gaps in the NO_x data reported by one group (Brookhaven National Laboratory (BNL)) were filled in by the NO_x data reported by the other group (NOAA) after these data had been properly adjusted. Gaps typically scattered during the course of a day ranged from 5 to 75 min and were always less than 30% of a total 24-hour period. Adjustments were made by linear regression of coincident 1 min data collected during any particular day, which seemed justified by the fact that both groups operated conceptually identical CD techniques. For example, 2338 coincident 1 min NO_x measurements were reported for the period June 30 to July 2, and the NOAA data were systematically 4% higher (slope of 1.04) and offset by 0.4 ppbv (intercept) at $r^2 = 0.92$, reflecting the precision of the specific NO_x CD measurement technique. No other, conceptually different technique was deployed during this experiment that would allow an assessment of the absolute accuracy. Our accuracy estimate of ±20% can be considered conservative based on numerous intercomparison studies [for example, *Gregory et al.*, 1990; *Fehsenfeld et al.*, 1990; *Harder et al.*, 1997], who compared distinctively different techniques to measure NO and NO_2.

Considering the inaccuracies of the measured input parameters $\sigma(X_i)$ from Table 1 and uncertainty estimates for k_1 = ±20% [*DeMore et al.*, 1994], and $j(NO_2)$ = ±30% from above, uncertainties of the calculated hourly averages of the gross ozone production rate were evaluated by propagation of errors, using

$$\sigma(P(O_3)) = \{\Sigma[(\sigma(X_i))^2 (\partial P(O_3)/\partial X_i)^2]\}^{1/2}. \quad (3)$$

The derivatives of $P(O_3)$ due to each independent variable (X_i) were derived analytically from equation (2) using hourly averages of the measured 1 min input variables that met the screening criteria above. The errors in $P(O_3)$ are expressed in percent of its absolute quantity as relative errors

$$\varepsilon(P(O_3)) = \pm \sigma(P(O_3)) / |P(O_3)| \times 100\%. \quad (4)$$

For the entire data set, $\varepsilon(P(O_3))$ averages at ±1700% with minimum at ±58%, while the average for the specific 3-day-period June 30 to July 2 is ±1330% with minumum ±137%. It is evident that the relative errors are smaller when $|P(O_3)|$ is significantly greater than 0, which was the case especially around noon and early afternoon. This can be seen in Figure 6a that shows $P(O_3)$ for the period June 30 to July 2, in comparison with other budget terms explained below. Figure 6b shows the difference between the production term $j(NO_2)[NO_2]$ and the loss term $k_1[O_3][NO]$ that make up $P(O_3)$, with absolute errors estimated from propagated errors of the individual hourly averaged measurements similar to equation (3). The relative errors in $P(O_3)$ according to equation (4) are depicted in Figure 6c on a lognormal scale. They averaged at ±2530% before noon, and at ±260% around noon and early afternoon. The errors in the production term shown in Figure 6b are always larger than the errors in the loss term, therefore indicating greater uncertainties in PSS-derived $P(O_3)$ induced by possible systematic errors in $j(NO_2)$. The additional uncertainty due to real atmospheric fluctuations in the measured variables during the averaged 1-hour intervals was a minor contributor to the overall error in $P(O_3)$.

The primary O_3 photochemical loss ($L(O_3)$ in equation (1)) in the southeastern U.S. troposphere during midday, clear-sky conditions is photolysis and subsequent reaction of $O^{(1D)}$ with H_2O to form OH [*Hauglustaine et al.*, 1996; *Frost et al.*,1998]. The 1 min O_3 photolysis rate constants, $j(O_3)$, were determined in the same manner as $j(NO_2)$. For the midday periods considered here, O_3 reactions with HO_2 and olefins were minor contributors to the total photochemical ozone loss rate $L(O_3)$. Their contributions relative to the primary O_3 photochemical loss were estimated at New Hendersonville based on the Rural Oxidanys in the Southern Environment (ROSE) study in Alabama [*Frost et al.*, 1998] since no radical nor VOC data were available from the 1994 New Hendersonville site. The uncertainty of this estimate of the total ozone loss rate amounted to ±50%.

An O_3 deposition rate L_{dep} was calculated by assuming a deposition velocity v_{dep} that would represent the larger region in the outflow of the Nashville urban plume and be valid for the average CBL encountered. Since ozone deposition to vegetation is stomatal-controlled, a diurnal character of v_{dep} was assumed. For the mostly deciduous forests in this region in summer, about 0.65 cm s^{-1} in the morning (0800 CST) increasing to a 1.2 cm s^{-1} peak around noon seemed reasonable [cf. *McMillan et al.*, this issue; *Padro*, 1993; *Hicks et al.*, 1989; *Lenschow et al.*, 1981; *Galbally and Roy*, 1980]. With the measured average CBL mixed height z_i and measured $[O_3]$, the ozone loss rate via surface deposition was estimated by

$$L_{dep} = v_{dep} [O_3] / z_i. \quad (5)$$

The uncertainty of v_{dep} was estimated from ozone flux measurements off an aircraft platform flying at an average 100 m agl during the 1995 SOS intensive [*McMillan et al.*, this issue]. The relative standard deviation (RSD) of v_{dep} determined as the average of zonally binned data from multiple consecutive 65 km flight legs across the Nashville urban plume during midday hours amounts to ~ ±40%. With an estimated uncertainty of ±15% for the wind profiler measurements of z_i under clear-sky conditions, the overall uncertainty of the O_3 deposition rate is better than ±43%.

The observed rate of O_3 change, $d[O_3]/dt$, was derived from the 1-min data by taking a finite difference derivative of the form

$$d[O_3(t_0)]/dt = ([O_3(t_0+30\text{ min})]-[O_3(t_0-30\text{ min})])/1\text{ hour} \quad (6)$$

averaged over the 1 hour intervals shown in Figure 6. Since the precision of the O_3 analyzer is ±2% at 100 ppbv, the uncertainty of the observed rate is estimated to be about ±3%.

An additional term was calculated according to equation (1) above by subtracting the net production ($P(O_3) + L(O_3) + L_{dep}$) from $d[O_3]/dt$. This residual term (T in equation (1)) is a result of all of the transport phenomena, such as advection, entrainment, and venting, that affect the O_3 mixing ratios at New Hendersonville. From the above error analysis it is obvious that the uncertainty in the derived transport term T is governed by the relatively large errors in $P(O_3)$ amounting to a minimum factor of 2.

As an approximation, the effects of advection on $[O_3]$ will be considered small compared to other transport effects. This

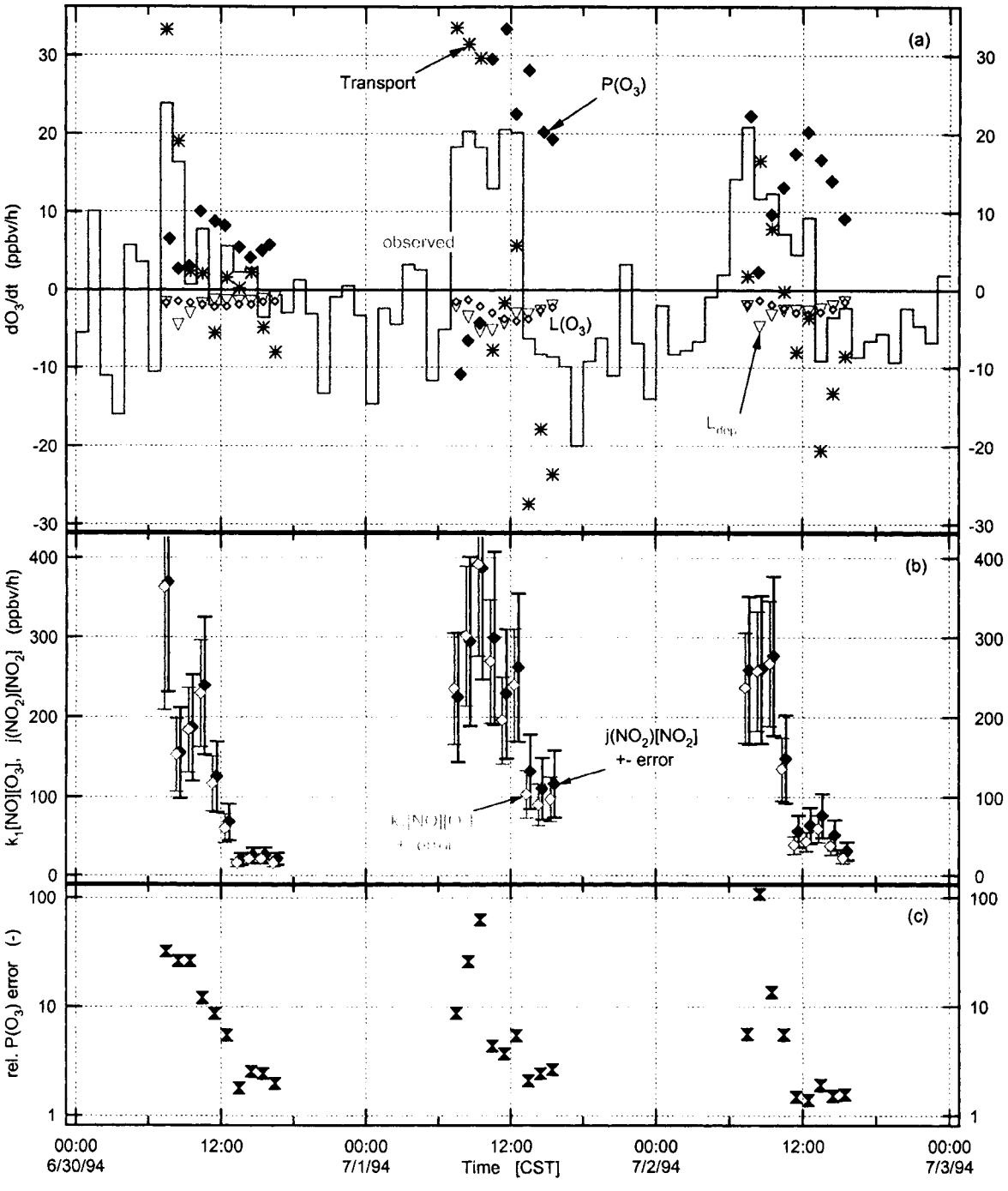

Figure 6. Hourly averages of (a) the observed rate of $[O_3]$ change compared to photochemical production $P(O_3)$, loss $L(O_3)$, deposition L_{dep}, and the derived transport term on July 1, 1994, and the 2 neighboring days for comparison with Plates 1 and 2 and Figure 5; (b) the individual production and destruction terms of $P(O_3)$ with propagated errors of the measured input variables similar to equation (3) (denoted "error"); and (c) relative uncertainty in $P(O_3)$ estimated from propagation of errors according to equation (3).

assumption is not unreasonable considering the fairly uniform distribution of O_3 throughout the region seen in Figure 5, especially during relatively calm morning hours. Now an estimate can be made for the effect of entrainment, which is a result of vertical mixing of the rapidly expanding boundary layer with free tropospheric air above. In many cases, the air above the boundary layer contains remnants of the boundary layer from the previous day, which can be subject to more vigorous advection and redistribution within that layer. Ozone "reservoir layers" established and conserved above nocturnal surface inversions have been shown in many airborne measurements in the past [e.g., *Paffrath*, 1988;

Ridley et al., 1998] and from P3-aircraft data collected particularly during this campaign with the only early morning takeoff on July 11, 1994, as shown in Figure 7. Entrainment of these air masses containing conserved and nondepleted O_3 from the photochemically active day before contributed to the rapid increases of $[O_3]$ near the surface during the first 2-3 hours after sunrise on July 1. On this day the phase of the most noticeable and effective vertical mixing was in the morning between 0700 and 1000 CST under still relatively slow CBL growth. As shown in Plate 1, this was the time of calm conditions (average wind speeds of 0.8 ±0.5 m s^{-1}) when advection likely contributed very little to the overall transport so that neglecting advection seemed justified. The resulting entrainment term, shown as the transport term in Figure 6, shows a large contribution to the observed $[O_3]$ change rate during this time. Applying this budget analysis under the same assumptions to the entire screened data set on the basis of diurnal averages leads to mean entrainment rates of 10-15 ppb h^{-1} between 0700 and 0900 CST [*Baumann et al.*, 1999].

Examination of this July 1 episode in more detail shows interesting features with respect to the behavior of $[O_3]$. Between 0300 and 0600 CST there was a light surface wind

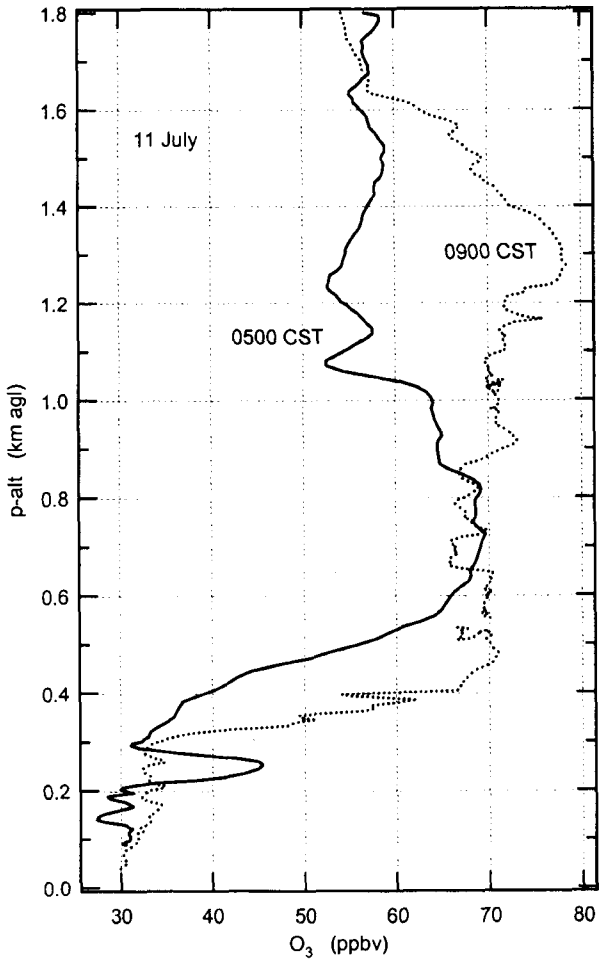

Figure 7. Vertical profiles of $[O_3]$ measured above the Nashville airport on board the NOAA WP-3D Orion research aircraft (P3) during takeoff at 0500 CST and landing at 0900 CST on July 11, 1994.

from the northeast (Plate 1). Levels of NO_x, NO_y, and CO (Plate 2) were fairly low until 0600 CST when the wind shifted to the east and the New Hendersonville site was influenced by emissions from a highway about 1 km to the east. Ozone was titrated essentially to zero (Figure 5). By 0800 CST the wind had shifted from the east to the southeast, and the site was influenced by a power plant plume containing high levels of SO_2 (Plate 2). This undoubtedly was the plume from Gallatin, located about 20 km to the east (Figures 1 and 4). As the wind continued to shift toward the southwest, the power plant plume passed by the site, but [CO] and the nitrogen oxides remained high (Plate 2). At 1000 CST it was apparent that the boundary layer had risen past 550 m agl since the surface wind direction then coincided with the wind direction aloft and the 550 m agl wind speed had dropped to the surface wind speed. During this period (0700-1000 CST), $[O_3]$ climbed steadily from ~5 to 80 ppbv, yet the O_3 production term was negative. Since there are no other sources of O_3 (neglecting advection), entrainment of $[O_3]$-rich air from above must be responsible for the increase at the surface. Moreover, from the data we can estimate what the O_3 level was aloft. At about 1100 CST there was a significant drop in the levels of CO, NO_y, and the individual NO_y species (Plate 2). There was also a drop in the H_2O mixing ratio, which corresponded to an extremely rapid increase in the CBL between 1100 and 1200 CST (Plate 1). However, the O_3 level remained almost constant during this period. It seems likely that the explosive growth of the CBL during this period resulted in rapid downward mixing of drier air containing levels of CO and NO_y that were much lower than the surface mixing ratios but about the same mixing ratio of O_3. Thus the O_3 levels aloft probably were about 80-85 ppbv, but since the aircraft was not flying on July 1 this cannot be confirmed. A periodic decoupling of the residual layer aloft from the nocturnal surface inversion can be seen by the traces of wind direction and speed at 10 and 550 m agl in Plate 1 (top). It seems reasonable, then, that air masses aloft with maximum ozone levels of 92 ppbv encountered by the P3 the afternoon before were relatively conserved and advectively redistributed overnight. A similar analysis of data on July 2 shows that $[O_3]$ leveled off at ~70 ppbv between 1000 and 1200 CST, and this value is in good agreement with the 65 ppbv measured at 1000 CST by the P3 at an altitude above 1.4 km agl, that is, above the CBL (Figure 8). Compared to June 30, the July 2 profile shows higher ozone levels in the residual layer indicating some remainder of the previous day's local ozone buildup and subsequent nocturnal advective redistribution.

It appears, then, that the buildup of $[O_3]$ at the surface prior to 1100 CST on July 1 was almost exclusively due to entrainment of $[O_3]$-rich air from aloft. Around this time the photochemical production term (Figure 6) became strongly positive, and $[O_3]$ continued a rapid increase, eventually reaching a peak of 125 ppbv at 1230 CST. During this late morning-early afternoon period the wind was from the south-southwest, and the site was influenced not only by the Nashville urban plume (20 km distant), but also by a major highway and a burning landfill (2 km distant). Thus the levels of NO_x and CO (and, presumably, AVOC) remained high, which is consistent with the calculated high $P(O_3)$ values (Figure 6). High levels of AVOC also appear to be indicated by the very high ratio (~0.2) of [PPN] to [PAN] (Plate 2).

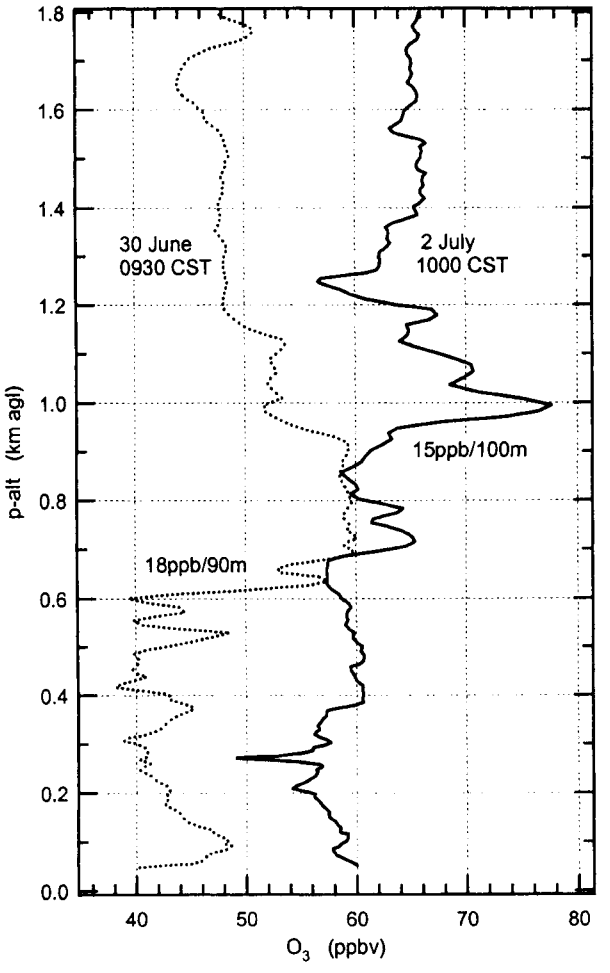

Figure 8. Vertical profiles of $[O_3]$ measured on board the NOAA WP-3D Orion research aircraft (P3) during takeoff from Nashville airport at 0930 CST on June 30 and 1000 CST on July 2, 1994.

The estimated entrainment rate was checked against other data as follows. Figure 8 shows the $[O_3]$ vertical profiles during the P3 aircraft takeoff from the Nashville airport at 0930 and 1000 CST on June 30 and July 2, respectively. The earlier ascent at 0930 CST on June 30 indicates the top of the CBL at 600 m agl, and an $[O_3]$ increase of 18 ppbv within 90 m above. At an estimated entrainment rate of 11 ppbv h^{-1} (average between 0900 and 1000 CST in Figure 6), the entrainment velocity, simply calculated as the ratio of the rate over the gradient, amounts to 1.5 cm s^{-1}. This same value can be determined for the July 2 profile where an ozone gradient of about 15 ppbv per 100 m is located at a CBL height of 900 m agl, and the 1000 CST entrainment rate averages at 8 ppbv h^{-1}. As mentioned above, an earlier research flight was conducted on July 11, with takeoff at 0500 and landing at 0900 CST. The morning of this day was sunny and dry, hence comparable to June 30. By 0900 CST, the CBL was about 300 m deep, with an almost uniform 33 ppbv of $[O_3]$ indicating fairly well mixed conditions. An approximately 800 m deep layer located ~180 m above the CBL contained $[O_3]$ relatively uniformly mixed at ~70 ppbv. This O_3 gradient pointed to a decoupling of the nocturnal inversion layer from the air aloft at night, conserving O_3 that had been photochemically produced the day before. The entrainment rate was determined in the same type budget analysis as above specifically for 0900 CST on July 11, and resulted in an average of 15 ppbv h^{-1}. Given the observed vertical $[O_3]$ gradient of ~37 ppbv over 180 m, an average O_3 entrainment velocity of 2 cm s^{-1} was calculated. This and the 1.5 cm s^{-1} velocity from above agree within 30 to 50% with entrainment velocity estimates of 3 ±1 cm s^{-1} that were derived from both wind profiling radar data and radiosonde data in a region with similar climatology [*Angevine et al.*, 1997, 1998]. The total relative error of the entrainment rate calculated here was determined from propagation of errors of the uncertainties that were used in the entrainment calculation (equation (1)) and amounted to 38 and 64% for the data on July 2 and June 30, respectively, when only instrumental uncertainties were considered. However, our assumptions for $L(O_3)$ did not include the close vicinity of anthropogenic pollution sources, and of course $P(O_3)$ is subject to the already mentioned errors associated with taking the difference between two large numbers. These factors are reflected largely in the variability of the 1 min data which if taken into account lead to fractional uncertainties of 1.75 for July 2 and 4.5 for June 30, mainly driven by the relative error in $P(O_3)$.

After 1400 CST on July 1, the New Hendersonville $[O_3]$ decreased even though the $P(O_3)$ term remained high until 1600 CST (compare Figures 5 and 6). The CBL had reached a maximum detectable height about 2 hours earlier (Plate 1), so dilution by mixing into a growing mixed volume was not reducing $[O_3]$. Also, the wind remained constant from the southwest between 1400 and 1700 CST indicating a relatively constant influence by advection, yet $[NO_y]$ and [CO] were decreasing almost exponentially (Plate 2). At this time, though, significant cloudiness was apparent (Plate 1) that reduced $j(NO_2)$ by about 30% compared to the values before noon. In addition to the reduced light levels, however, it is possible that cloud venting might have contributed substantially to this steep O_3 decrease in that it provided the mechanism to effectively dilute the local ozone exceedance down to ozone levels that represented more regional character by 1800 CST. Cloud venting, that is, the upward air mass transport from the CBL to higher altitudes and its temporal and spatial evolution and scale, are currently investigated [cf. *Angevine et al.*, 1998]. This vertical convective transport is associated with the occurrence of broken cumulus clouds, which typically appeared in the afternoon at the site. On July 2 at 1000 CST the P3 measured an average 65 ppbv $[O_3]$ between 1.4 and 3 km agl, well above the still evolving CBL (Figure 8). If we considered this an upper limit of "free tropospheric" ozone during the afternoon of July 1, we can estimate vertical O_3 venting velocities v_{vent}. Ceilometer data and aerosol-backscatter determined by a differential-absorption lidar (DIAL) system that began operation at Rayon City on July 1 helped to identify the average base and top of the occurring broken cloud cover: this layer Δz was approximately 1000 m deep (A. B. White, personal communication, 1997). Considering well-mixed conditions up to cloud base, vertical ozone gradients ($\Delta[O_3]/\Delta z$) can be estimated by the difference between the surface measurements at New Hendersonville and the "free troposphere" level of 65 ppbv. Assuming that the transport term T at 1300-1600 CST on July 1, shown in Figure 6, is

mainly driven by cloud venting, a venting velocity can be derived by $v_{vent} = T / (\Delta[O_3]/\Delta z)$. At the observed rates the approximate ozone vertical venting velocities ranged from 11 to 16 cm s^{-1}. This process seems to effectively remove ozone from the CBL into higher altitudes and needs further investigation by comparison with other loss mechanisms, for example, surface deposition, in future work.

6. Summary and Conclusions

The high O_3 episode for the New Hendersonville site did not result in an official violation of the NAAQS standard of 120 ppbv because this was not an EPA-sanctioned air monitoring site. Nevertheless, it is clear that a violation occurred, and there are sufficient data to examine why the episode (and apparent violation) occurred. There is little doubt that a large contributing factor to the high $[O_3]$ on July 1 was the presence of high $[O_3]$ aloft. The increase of $[O_3]$ from essentially 0 ppbv to about 80 ppbv from 0700 to 1000 CST can only reasonably be explained by entrainment of $[O_3]$-rich air into the rising CBL since photochemical production was virtually nonexistent during this period. The combined analysis of the meteorological and chemical data indicates that this $[O_3]$-rich air is the remnant of the previous day's local ozone buildup and subsequent nocturnal advective redistribution. There is equally little doubt that the "push" required for O_3 levels to exceed the NAAQS standard of 120 ppbv in 1 hour (or the newer standard of 80 ppbv over 8 hours) was provided by intense photochemical O_3 production in the Nashville urban plume as it passed over the New Hendersonville site. The fact that O_3 did not peak nearly as high the next day is most likely due to the urban plume being blown away from the New Hendersonville site between 1000 and 1100 CST. Plate 2 shows that at midmorning of July 2 there was more than sufficient $[NO_x]$ and, probably, [AVOC] (reflected in high [CO] and high [PPN]/[PAN]) to photochemically produce O_3 at levels seen the previous day. However, when the wind shifted from southwesterly to southerly or southeasterly, there was a sudden drop in the mixing ratios of these species, the photochemistry was not as vigorous, and $[O_3]$ peaked at just over 80 ppbv resulting in no apparent NAAQS violation. It is highly probable that areas to the north and northwest of Nashville experienced a high $[O_3]$ episode on July 2, although we do not have the data to confirm this since no ground monitoring was conducted in those areas for this study. The specific characteristics of plume transport and dispersion indicate that a denser monitoring network would result in an increased number of reported ozone violations during summertime stagnation periods around Nashville.

The fact that entrainment of O_3 from aloft provides such a large proportion of surface $[O_3]$ cannot be neglected, but the factors that are responsible for this are quite complex and varied. There is no doubt the O_3 produced throughout the CBL on the previous day (or days) contributes, but since nocturnal boundary layers generally strongly decouple the surface from the free troposphere, advective motion of these layers aloft at night and early mornings around large regions must be taken into account. Analysis of the July 1 episode also indicates that the emissions of photochemical precursors from upwind locations can seriously degrade air quality downwind on subregional scales. In summary, high $[O_3]$ produced at a particular ground location may not only be due to emissions being imported during the day to drive photochemical production, but those high surface O_3 levels may also be due to O_3 being imported into the region during nighttime and early morning hours. These are the important scientific and policy issues that require further study.

Acknowledgements. We appreciated the help provided by TVA, Muscle Shoals, in particular Jessica Christ, Ken Olszyna, Bill Parkhurst, and Roger Tanner who furnished EPA Level 1 ozone data. Donna Sueper, NOAA-AL, Boulder, helped with the wind profiles illustration in Figure 3. Tom Jobson, Paul Murphy, Tom Ryerson, Michael Trainer, and Jonathan Williams, all NOAA-AL, and Brian Ridley, NCAR, Boulder, largely contributed to this work in fruitful discussions. Special thanks go to Gerd Hübler and David Parrish, NOAA-AL, for providing P3 aircraft data, and to Margaret Pippin, Univ. of Michigan, for her support in the field. This research was partly funded by the NOAA Climate and Global Change Program.

References

Angevine, W.M., A.B. White, and S.K. Avery, Boundary-layer depth and entrainment zone characterization with a boundary-layer profiler, *Boundary Layer Meteorol., 68*, 375-385, 1994a.

Angevine, W.M., et al., Wind profiler mixing depth and entrainment measurements with chemical applications, paper presented at 8th Joint Conference on Applications of Air Pollution Meteorology, Air and Waste Manage. Assoc., Nashville, Tenn., 1994b.

Angevine, W.M., et al., Entrainment results from the Flatland boundary layer experiments, paper presented at 12th Symposium on Boundary Layers and Turbulence, Amer. Meteorol. Soc., Vancouver, B. C., Canada July 28 to Aug. 1, 1997.

Angevine, W.M., et al., Entrainment results from the Flatland boundary layer experiments, *J. Geophys. Res., 103*, 13,689-13,701, 1998.

Atkinson, R., Gas-phase tropospheric chemistry of organic compounds: A review, *Atmos. Environ., Part A, 24*, 1-41, 1990.

Baumann, K., et al., Ozone photochemistry and transport of the Nashville urban plume during the 1994 Southern Oxidants Study (SOS), guest contribution, in *Proceedings of EUROTRAC Symposium'98*, edited by P.M. Borrell and P. Borrell, pp. 855-861, WIT Press, Southampton, England 1999.

Chameides, W.L., et al., Observed and model-calculated NO_2/NO ratios in tropospheric air sampled during the NASA GTE/CITE2 field study, *J. Geophys. Res., 95*, 10,235-10,247, 1990.

Cleveland, W.S., et al., Geographical properties of ozone concentrations in the northeastern United States, *J. Air Pollut. Control Assoc., 27*, 325-328, 1977.

Dahlback, A., and K. Stamnes, A new spherical model for computing the radiation field available for photolysis and heating at twilight, *Planet. Space Sci., 39*, 671-683, 1991.

DeMore, W.B., et al., Chemical kinetics and photochemical data for use in stratospheric modeling, *Evaluation 11, JPL Publ. 94-26*, 1994.

Environmental Protection Agency (EPA), The 1985 NAPAP Emissions Inventory (Version 2): Development of the National Utility Reference File, *EPA-600/7-89-012a, -013a*, Washington, D. C., 1989.

Fahey, D.W., et al., Reactive nitrogen species in the troposphere: Measurements of NO, NO_2, HNO_3, particulate nitrate, peroxyacetyl nitrate (PAN), O_3, and total reactive odd nitrogen (NO_y) at Niwot Ridge, Colorado, *J. Geophys. Res., 91*, 9781-9793, 1986.

Fehsenfeld, F.C., et al., A study of ozone in the Colorado mountains, *J. Atmos. Chem., 1*, 87-105, 1983.

Fehsenfeld, F.C., et al., Intercomparison of NO_2 measurement techniques, *J. Geophys. Res., 95*, 3579-3597, 1990.

Frost, G.J., et al., Photochemical ozone production in the rural southeastern United States during the 1990 Rural Oxidants in the Southern Environment (ROSE) program, *J. Geophys. Res., 103*, 22,491-22,508, 1998.

Galbally, I.E., and C.R. Roy, Destruction of O_3 at the Earth's surface, *Q. J. R. Meteorol. Soc., 97*, 18-29, 1980.

Gregory, G.L., et al., An intercomparison of airborne nitric oxide measurements: A second opportunity, *J. Geophys. Res., 95*, 10,129-10,138, 1990.

Harder, J.W., E.J. Williams, K. Baumann, and F.C. Fehsenfeld, Ground-based comparison of NO_2, H_2O, and O_3 measured by long-path and in situ techniques during the 1993 Tropospheric OH Photochemistry Experiment, *J. Geophys. Res., 102*, 6227-6243, 1997.

Hauglustaine, D.A., et al., Observed and model-calculated photostationary state at Mauna Loa Observatory during MLOPEX 2, *J. Geophys. Res., 101*, 14,681-14,696, 1996.

Hicks, B.B., D.R. Matt, and R.T. McMillen, A micrometeorological investigation of surface exchange of O_3, SO_2 and NO_2: A case study, *Boundary Layer Meteorol., 47*, 321-336,1989.

Kelly, N.A., et al., Trace gas and aerosol measurements at a remote site in the northeast United States, *Atmos. Environ., 18*, 2565-2576, 1984.

Kleinman, L., et al., Peroxy radical concentration and ozone formation rate at a rural site in the southeastern United States, *J. Geophys. Res., 100*, 7263-7273, 1995.

Kley, D., and M. McFarland, Chemiluminescence detector for NO and NO_2, *Atmos. Technol.,12*, 63-69, 1980.

Lenschow, D.H., R. Pearson Jr., and B.B. Stankov, Estimating the ozone budget in the boundary layer by use of aircraft measurements of ozone eddy flux and mean concentration, *J. Geophys. Res., 86*, 7291-7297, 1981.

Liu, S.C., et al., Ozone production in the rural troposphere and the implications for regional and global ozone distributions, *J. Geophys. Res., 92*, 4191-4207, 1987.

McMillen, R.T., R.L. Gunter, W.T. Luke, and T.B. Watson, Ozone fluxes obtained with the NOAA Twin Otter during the Southern Oxidants Study, *J. Geophys. Res.*, this issue.

Meagher, J.F., E. B. Cowling, F. C. Fehsenfeld, and W. J. Parkhurst, Ozone formation and transport in the southeastern United States: An overview of the SOS Nashville/Middle Tennessee Ozone Study, *J. Geophys. Res., 103*, 22,213-22,223, 1998.

National Research Council (NRC), *Rethinking the Ozone Problem in Urban and Regional Air Pollution*, Natl. Acad. Press, Washington, D. C., 1991.

Norton, R.B., et al., Measurements of nitric acid and aerosol nitrate at the Mauna Loa Observatory during the Mauna Loa Observatory Photochemistry Experiment 1988, *J. Geophys. Res., 97*, 10,415-10,425, 1992.

Padro, J., Seasonal contrasts in modeled and observed dry deposition velocities of O_3, SO_2 and NO_2 over three surfaces, *Atmos. Environ., Part A, 27*, 807-814, 1993.

Paffrath, D., Untersuchung über die Verteilung und Bildung von Ozon im Alpenbereich aus Flugzeugmessungen, *Verteilung und Wirkung von Photooxidantien im Alpenraum*, edited and published by GSFmbH München, 242-251, 1988.

Parrish, D.D., et al., Measurements of the NO_x-O_3 photostationary state at Niwot Ridge, Colorado, *J. Geophys. Res., 91*, 5361-5370, 1986.

Parrish, D.D., J.S. Holloway, and F.C. Fehsenfeld, Routine, continuous measurement of carbon monoxide with parts per billion precision, *Environ. Sci. Technol., 28*, 1615-1618, 1994.

Peeters, J., J. Vertommen, and I. Langhans, Rate constants of the reactions of CF_3O_2, i-$C_3H_7O_2$ and t-$C_4H_9O_2$ with NO, *Ber. Bunsen Ges. Phys. Chem., 96*, 431-436, 1992.

Research Triangle Institute (RTI), Investigation of rural oxidant levels as related to urban hydrocarbon control strategies, *EPA-450/3-75-036*, 359 pp., Environ. Prot. Agency, Research Triangle Park, N. C., 1975.

Ridley, B.A., et al., Measurements and model simulations of the photostationary state during the Mauna Loa Observatory Photochemistry Experiment: Implications for radical concentrations and ozone production and loss rates, *J. Geophys. Res., 97*, 10,375-10,388, 1992.

Ridley, B.A., et al., Measurements of reactive nitrogen and ozone to 5-km altitude in June 1990 over the southeastern United States, *J. Geophys. Res., 103*, 8369-8388, 1998.

Roberts, J.M., et al., Measurements of PAN, PPN, and MPAN made during the 1994 and 1995 Nashville intensives of the Southern Oxidants Study: Implications for regional ozone production from biogenic hydrocarbons, *J. Geophys. Res., 103*, 22,473-22,490, 1998.

Shetter, R.E., et al., Actinometer and Eppley radiometer measurements of the NO_2 photolysis rate coefficient during the Mauna Loa Observatory Photochemistry Experiment, *J. Geophys. Res., 97*, 10,349-10,359, 1992.

Spicer, C.W., et al., Ozone sources and transport in the northeastern United States, *Environ. Sci. Technol., 13*, 975-985, 1979.

St. John, J.C., and W.L. Chameides, Climatology of ozone exceedences in the Atlanta metropolitan area: 1-hour vs. 8-hour standard and the role of plume recirculation air pollution episodes, *Environ. Sci. Technol., 31*, 2797-2804, 1997.

Vukovich, F.M., et al., On the relationship between high ozone in the rural surface layer and high pressure systems, *Atmos. Environ., 11*, 967-983, 1977.

Vukovich, F.M., J. Fishman, and E.V. Browell, The reservoir of ozone in the boundary layer of the eastern United States and its potential impact on the global tropospheric ozone budget, *J. Geophys. Res., 90*, 5687-5698, 1985.

White, A.B., Mixing depth detection using 915-Mhz radar reflectivity data, paper presented at 8th Symposium on Observations and Instrumentation, Am. Meteorol. Soc., Boston, Mass., 1993.

Williams, E.J., et al., Variations in NO_y composition at Idaho Hill, Colorado, *J. Geophys. Res., 102*, 6296-6314, 1997.

Williams, E.J., et al., Intercomparison of ground-based NO_y measurement techniques, *J. Geophys. Res., 103*, 22,261-22,280, 1998.

Williams, J., et al., Regional ozone from biogenic hydrocarbons deduced from airborne measurements of PAN, PPN, and MPAN, *Geophys. Res. Lett., 24*, 1099-1102, 1997.

Wolff, G.T., and P.J. Lioy, Development of an ozone river associated with synoptic scale episodes in the eastern United States, *Environ. Sci. Technol., 14*, 1257-1260, 1980.

W. M. Angevine, F. C. Fehsenfeld, G. J. Frost, R. B. Norton, J. M. Roberts, and E. J. Williams, Aeronomy Laboratory, National Oceanic and Atmospheric Administration, R/E/AL7, 325 Broadway, Boulder, CO 80303. (wayne@al.noaa.gov; eric@al.noaa.gov).

K. Baumann, School of Earth and Atmospheric Sciences, Georgia Institute of Technology, 221 Bobby Dodd Way, OCE 205, Atlanta, GA 30332-0340. (kb@eas.gatech.edu).

S. B. Bertman, Department of Chemistry, Western Michigan University, Kalamazoo, MI 49008.

B. Hartsell, Atmospheric Research and Analysis, Inc., 4429 Cityview Drive, Plano, TX 75093.

S. R. Springston, Environmental Chemistry Division, Brookhaven National Laboratory, P.O. Box 5000, Upton, NY 11973-5000.

(Received January 12, 1999; revised September 27, 1999; accepted September 28, 1999.)